Article
DOI: 10.1002/bkcs.11911

BULLETIN OF THE
KOREAN CHEMICAL SOCIETY

Syntheses of 1,1-Diethyl- or -Dihexyl-3,4-Diphenyl-2,5-Dibromo- or -Bis (Trimethylsilyl)Siloles and Electrochemical Properties for Lithium Ion Battery

Ji Young Park,[†] Young Min Jung,[‡] and Young Tae Park[†],[*]

[†]*Department of Chemistry, Keimyung University, Daegu 42601, South Korea.*
**E-mail: ytpark@kmu.ac.kr*
[‡]*Division of Green Energy Research, Daegu Gyeongbuk Institute of Science and Technology, Daegu 42988, South Korea*

Received August 20, 2019, Accepted October 21, 2019

1,1-Diethyl- and 1,1-dihexyl-3,4-diphenyl-2,5-dibromosiloles (**3a** and **3b**, respectively) as well as 1,1-diethyl- and 1,1-dihexyl-3,4-diphenyl-2,5-bis(trimethylsilyl)siloles (**4a** and **4b**, respectively) were prepared by intramolecular reductive cyclization and bromination or trimethylsilylation of diethyl- or dihexyl-bis(phenylethynyl)silanes (**2a** and **2b**), respectively. The IR stretching frequencies for all the synthesized silole derivatives appeared within the range 1543–1566 cm^{-1}. The UV–vis absorption data of the siloles in THF include absorption peaks at 303–326 nm, with molar absorptivities ranging from 2.63×10^3 to 5.99×10^3 L/(cm·mol). In the excitation spectra, maximum excitation bands were found at 355–371 nm, while maximum emission peaks in the fluorescence spectral data were observed at 419–443 nm. Cyclic voltammograms (CVs) of **3a** and **3b** revealed oxidation peaks at 0.16 and 0.58 V, and reduction peaks at −0.25 and − 0.28 V, respectively. Meanwhile, CVs of **4a** and **4b** showed two oxidation peaks between −0.46 and 0.14 V, and two reduction peaks between −1.32 and − 0.69 V, respectively. Thermogravimetric ananysis (TGA) experimental data illustrated that all the synthesized siloles were thermally stable at temperatures up to 150 °C with only 0.3–3% loss of their original masses under nitrogen. The long cycling performance of anodes **4a** and **4b,** at 1.0 A/g current density, exhibited initial discharge/charge capacities of 1967/754 and 5559/1174 mAh/g with Coulombic efficiencies of 38.2 and 21.1% after 20 and 15 cycles, respectively.

Keywords: 1,1-Diethyl or 1,1-dihexyl-3,4-diphenyl-2,5-dibromosilole, 1,1-Diethyl or 1,1-dihexyl-3,4-diphenyl-2,5-bis(trimethylsilyl)silole, Photoelectronic characterizations, Electrochemical properties

Introduction

Silole has a skeleton of 1-silacyclopenta-2,4-diene,[1] which is a heterocyclic diene, and contains an unusual π-electronic system resulting in a lowest unoccupied molecular orbital energy level much lower than, for example, cyclopenta-2,-4-diene by 1.289 eV.[2] This is attributed to σ*–π* conjugation originating from an interaction between the silylene σ* orbital and the butadiene π* orbital.[3]

Silole derivatives bearing such a π-conjugated structure have been intensively studied for electronic device applications due to their unique electronic properties.[4–7] From the viewpoint of basic electrochemistry, siloles-containing π-conjugated materials have also attracted significant attention for their application in electroluminescence,[6,8–12] photoluminescence,[13–18] and organic field-effect transistors.[19] Dendrimers end-capped with siloles exhibit blueish green fluorescence emission, suggesting these materials may be useful for electroluminescent devices.[20]

Conjugated polymeric materials bearing silacyclopenta-2,4-diene, *i.e.*, silolene, are prepared by several different synthetic methods.[21–23] We previously published the syntheses of silole-bearing π-conjugated materials, such as poly(3,4-diphenyl-1,1-disubstituted-2,5-silole)s, via Grignard metathesis polymerization of 2,5-dibromo-3,4-diphenyl-1,1-disubstituted-siloles using the Grignard reagent.[24] In addition, we have studied the syntheses and electrochemical characteristics (*e.g.*, cyclic voltammogram [CV]) of poly[(3,4-diphenyl-1,1-disubstituted-2,5-silolene)-*co*-(disubstituted-silylene)]s bearing the 2,5-silolene and silylene moieties using *n*-butyllithium.[25]

We have also been interested in the synthesis and properties of poly(carbosilagermane)s contained within chromophores of 3,4-diphenyl-2,5-silolene and disubstituted-germylene, for example, poly[(1,1-diethyl-3,4-diphenyl-2,5-silolene)-*co*-(disubstitutedgermylene)]s.[26]

Energy storage systems, such as the lithium-ion battery, have received considerable interest due to their wide use in electronics and electric vehicles.[27,28] Recently, organic electrode materials have emerged as popular alternatives to inorganic materials and carbon-involved composites, for next generation lithium-ion batteries.[29,30]

The synthesis, as well as photoelectronic and electrochemical properties, of carbosilanes containing siloles have been studied in many ways thus far.[31–33] To our knowledge, there have not been any previous reports on the electrochemical properties, such as long cycling performance of anode materials, for silole derivatives like **4a** and **4b,** and their application to the lithium ion battery.

Herein, we report the synthesis of 1,1-diethyl- and 1,1-dihexyl-3,4-diphenyl-2,5-dibromosiloles (**3a** and **3b**, respectively) as well as 1,1-diethyl and -dihexyl-3,-4-diphenyl-2,5-bis(trimethylsilyl)siloles (**4a** and **4b**, respectively). In addition, photoelectronic characteristics (excitation, absorption, and emission spectra in the solution phase), thermal properties (utilizing thermogravimetric ananysis [TGA] method), and their electrochemical properties (CVs and long cycling performance of active anodes) are reported for the first time.

Experimental Section

General. All chemicals used for the experiments were purchased from Sigma-Aldrich Company Sigma-Aldrich Korea Corporation (Seoul, Korea). All the glassware used was set up, then flame-dried utilizing a burner under a stream of argon prior to experiments. All solvents were distilled before use according to methods reported in the literature.[34] For example, tetrahydrofuran was distilled from fine chopped sodium metal along with benzophenone ketyl prior to use.[34] ^{1}H and ^{13}C nuclear magnetic resonance (NMR) spectral data were collected using a JEOL 500 MHz FT-NMR spectrometers (Tokyo, Japan) using $CDCl_3$ as the solvent. Chemical shifts in all the NMR spectra were measured utilizing the residual proton peak of $CDCl_3$ and tetramethylsilane (TMS) as an internal standard. Infra-red spectroscopy was performed using a Thermo Scientific FT-IR iD50 spectrophotometer (Milwaukee, WI, USA) fourier transform - infrared spectroscopy (FT-IR) iD50 spectrophotometer. Ultraviolet-visible (UV–vis) absorption experiments were carried out using a Hewlett Packard 8453 spectrophotometer (USA). We recorded the excitation and fluorescence emission spectra using a fluorescence spectrophotometer from Horiba Fluorolog-3-11 fluorescence spectrophotometer (Edison, NJ, USA). We conducted cyclic voltammetry using a Bio-Logic Science Instrument, model VSP, Potentiostat (Claix, France) with a three-electrode cell system comprised of a platinum wire counter electrode, Ag/AgCl reference electrode, and copper working electrode with a potential window from +2 to −2 V. We prepared the working electrode by dipping the copper electrode in a hexane solution containing each synthesized silole derivative, followed by removal of the solvent via evaporation using a dry oven. We examined thermal properties of the obtained silole materials utilizing a thermal analysis instrument from Shimadzu TGA-50 (Kyoto, Japan). For these studies, we incrementally increased the temperature of the TGA from 25 to 900 °C with a heating rate of 10 °C/min in a nitrogen atmosphere applied at a 20 mL/min flushing rate. Cell properties obtained using charge/discharge experiments performed using a WonATech Multichannel Potentiostat/Galvanostat WMPG-1000 (Seoul, Korea).

Diethylbis(phenylethynyl)silane (2a). Diethylbis(phenylethynyl)silane (**2a**) was prepared by treatment of dichlorodiethylsilane (**1a**) with phenylacetylene using *n*-butyllithium in accordance with a published method.[24,35] A yellowish viscous liquid **2a** (26.0 g, 96.3%) was obtained quantitatively. ^{1}H NMR (500 MHz, $CDCl_3$): δ 0.90–0.95 (q, J = 7.8 Hz, 4H), 1.21–1.24 (t, J = 7.7 Hz, 6H), 7.32–7.38 (m, 6H), 7.55–7.57 (m, 4H). ^{13}C NMR (125 MHz, $CDCl_3$): δ 6.507, 7.313, 88.749, 106.631, 122.642, 128.132, 128.747, 132.077. ^{29}Si NMR (99 MHz, $CDCl_3$): δ −30.712. IR (neat) $\tilde{\nu}_{max}$: 3080, 3057, 3032, 2956, 2933, 2913, 2874, 2157 ($\nu_{C\equiv C}$), 1008, 965, 915, 831, 754, 723, 686 cm^{-1}.

Dihexylbis(phenylethynyl)silane (2b). Dihexylbis(phenylethynyl)silane (**2b**) was prepared by the treatment of dichlorodihexylsilane (**1b**) with phenylacetylene using *n*-butyllithium in accordance with a published method.[24,35] A yellowish viscous liquid **2b** (35.0 g, 94.0%) was obtained quantitatively. ^{1}H NMR (500 MHz, $CDCl_3$): δ 0.8–1.66 (m, 26H), 7.27–7.42 (m, 6H), 7.42–7.60 (m, 4H). ^{13}C NMR (125 MHz, $CDCl_3$): δ 14.148, 14.810, 22.604, 23.670, 31.521, 32.731, 89.469, 106.535, 122.843, 128.171, 128.737, 132.145. ^{29}Si NMR (99 MHz, $CDCl_3$): δ −34.697. IR (neat) $\tilde{\nu}_{max}$: 3079, 3057, 3032, 2955, 2921, 2854, 2158 ($\nu_{C\equiv C}$), 1099, 1068, 1026, 995, 958, 913, 832, 753, 687 cm^{-1}.

2,5-Dibromo-1,1-diethyl-3,4-diphenyl-silole (3a). 2,5-Dibromo-1,1-diethyl-3,4-diphenyl-silole (**3a**) was synthesized via intramolecular reductive cyclization of the compound **2a,** followed by bromination according to the literature.[24,35] A pale brownish powder **3a** (3,40 g, 32.5%) was obtained. ^{1}H NMR (500 MHz, $CDCl_3$): δ 1.04–1.09 (q, J = 7.8 Hz, 4H), 1.18–1.21 (t, J = 7 Hz, 6H), 7.00–7.02 (m, 4H), 7.17–7.22 (m, 6H). ^{13}C NMR (125 MHz, $CDCl_3$): δ 1.477, 6.536, 120.770, 127.355, 127.499, 128.948, 137.040, 157.216. ^{29}Si NMR (99 MHz, $CDCl_3$): δ 8.521. IR (neat) ν_{max}: 3026, 3055, 2962, 2930, 2908, 2877, 1566 ($\nu_{C=C}$), 1076, 1064, 1022, 953, 933, 912, 764, 729, 693, 637 cm^{-1}.

2,5-Dibromo-1,1-dihexyl-3,4-diphenyl-silole (3b). 2,5-Dibromo-1,1-dihexyl-3,4-diphenyl-silole (**3b**) was synthesized via intramolecular reductive cyclization of the compound **2b,** and bromination according to the literature.[24,35] A pale brownish powder **3b** (3.00 g, 31.9%) was obtained. ^{1}H NMR (500 MHz, $CDCl_3$): δ 0.91–1.01 (m, 10H), 1.23–1.58 (m, 16H), 6.95–6.97 (m, 4H), 7.15–7.19 (m, 6H). ^{13}C NMR (125 MHz, $CDCl_3$): δ 9.684, 14.148, 22.575, 22.854, 31.416, 32.683, 121.826, 127.345, 127.518, 128.948, 137.155, 156.775. ^{29}Si NMR (99 MHz, $CDCl_3$): δ 6.176. IR (neat) $\tilde{\nu}_{max}$: 3024, 3057, 2953, 2922, 2853, 1557 ($\nu_{C=C}$), 1075, 1060, 1025, 952, 766, 697 cm^{-1}.

2,5-Bis(trimethylsilyl)-1,1-diethyl-3,4-diphenyl-silole (4a). 2,5-Bis(trimethylsilyl)-1,1-diethyl-3,4-diphenyl-silole

(**4a**) was synthesized via intramolecular reductive cyclization of the compound **3a**, and trimethylsilation according to the literature.[8,24,35] A pale brownish powder product **4a** (5.00 g, 49.5%) was obtained. ^{1}H NMR (500 MHz, CDCl$_3$): δ −0.16 (s, 18H), 0.92–0.96 (m, 4H), 0.98–1.01 (m, 6H), 6.82–6.84 (m, 4H), 6.99–7.03 (m, 6H). ^{13}C NMR (125 MHz, CDCl$_3$): δ 0.470, 5.211, 7.285, 125.934, 126.865, 128.833, 141.628, 143.087, 171.077. ^{29}Si NMR (99 MHz, CDCl$_3$): δ −10.04, 29.90. IR (neat) $\tilde{\nu}_{max}$: 3022, 3057, 2951, 2895, 2873, 1543 ($\nu_{C=C}$), 1071, 1034, 1006, 952, 914, 831, 776, 753, 695, 684 cm^{-1}.

2,5-Bis(trimethylsilyl)-1,1-dihexyl-3,4-diphenyl-silole (4b). 2,5-Bis(trimethylsilyl)-1,1-dihexyl-3,4-diphenyl-silole (**4b**) was synthesized via intramolecular reductive cyclization of the compound **2b**, and trimethylsilation according to the literature.[8,24,35] A pale brownish powder product **4b** (5.00 g, 54.4%) was obtained. ^{1}H NMR (500 MHz, CDCl$_3$): δ −0.15 (s, 18H), 0.88–1.02 (m, 10H), 1.27–1.44 (m, 16H), 6.79–6.90 (m, 4H), 6.96–7.11 (m, 6H). ^{13}C NMR (125 MHz, CDCl$_3$): δ 0.642, 13.620, 14.196, 22.710, 23.890, 31.675, 33.172, 125.915, 126.846, 128.766, 142.732, 143.058, 170.520. ^{29}Si NMR (99 MHz, CDCl$_3$): δ −10.20, 26.56. IR (neat) $\tilde{\nu}_{max}$: 3057, 3021, 2953, 2916, 2850, 1545 ($\nu_{C=C}$), 1467, 1242, 1043, 1003, 954, 913, 831, 779, 756, 698 ($v_{Si–C}$) cm^{-1}.

Fabrication of Anode for Lithium Ion Batteries. Upon mixing the active material (**4a** or **4b**) with conductor super P, and binder polyvinylidenefluoride at an appropriate ratio, the mixture was stirred using a zirconia ball-milling in *N*-methylpyrrolidone for 24 h. The resulting well-mixed solution of electrode material was coated onto the current collector Cu foil using a doctor blade, and vacuum-dried under increasing temperature conditions from 50 to 110 °C over a 12-h period. The cell assembly of a 2032 type coin cell for the measurement of electrochemical properties, was performed inside a glove box under Argon atmosphere. Batteries were fabricated as half cells and the prepared active materials were employed as the working electrode. Lithium (Li) metal was used as the counter electrode, and polypropylene (PP) was used as the separator. The electrolyte solution contained 1.0 M LiPF$_6$ in ethylene carbonate and dimethyl carbonate at a 3:7 (vol.%) ratio.

The absorption, excitation, fluorescence emission data, TGA thermogram traces and CVs for **3a**, **3b**, **4a**, and **4b** along with the long cycling performance data for **4a** and **4b** are described below.

Results and Discussion

Synthesis. Scheme 1 illustrates the preparation of 1,1-diethyl- **(3a)** and 1,1-dihexyl-2,5-dibromo-3,4-diphenyl-1-silole (**3b**) using the two-step reaction protocol reported previously.[3,24] Dichlorodiethyl- (**1a**) or dihexylsilane (**1b**) were treated with lithium phenylacetylide, prepared *in situ* in THF via the reaction of ethynylbenzene with *n*-butyllithium, to obtain diethyl- (**2a**) or dihexylbis(phenylethynyl)silane **(2b).** Subsequently, reductive intramolecular cyclization of **2a** and **2b** using Li$^+$Naphth$^-$, anhyd. ZnCl$_2$, and NBS afforded **3a** and **3b**, respectively. The identity of **3a** and **3b** were confirmed using several spectroscopic methods, including NMR and IR studies. Some spectroscopic properties of compounds **3a**, **3b**, **4a**, and **4b** are listed in Table 1. The ^{1}H NMR spectra of **3a** and **3b** illustrate multiplet peaks at 1.04–1.21 and 0.91–1.58 ppm, due to the presence of C$_2$H$_5$ and C$_6$H$_{13}$ groups, respectively.[35–37] The ^{13}C NMR spectra of **3a** and **3b**, reveal two carbon peaks at 1.48 and 6.54 ppm due to the C$_2$H$_5$ group directly bound to the silole Si atom, and six carbon peaks between 9.68 and 32.68 ppm due to the C$_6$H$_{13}$ group directly bound to the silole Si atom.[35–37] In the ^{29}Si NMR spectra of **3a** and **3b**, the silicon peaks were found at 8.52 and 6.18 ppm, respectively.[38]

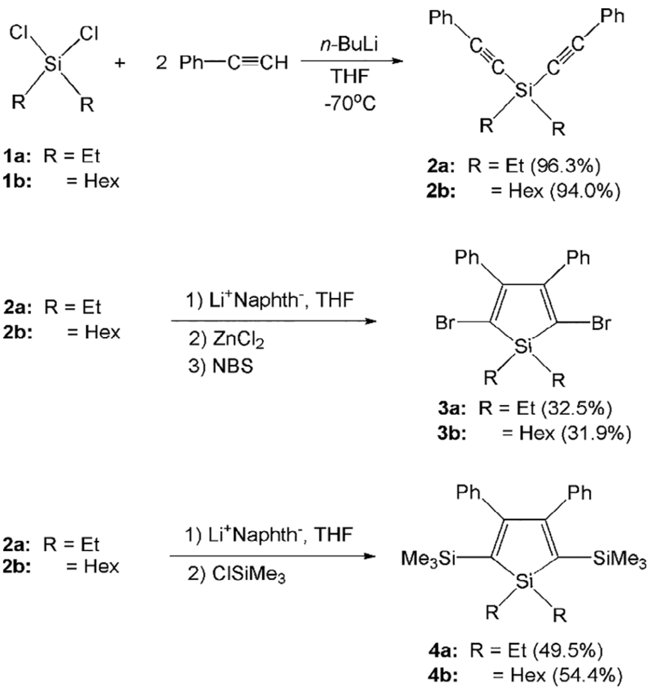

Scheme 1. Synthesis of siloles **3a**, **3b**, **4a**, and **4b**.

Scheme 1 also illustrates the synthesis of 2,5-bis(trimethylsilyl)-1,1-diethyl- (**4a**) and -dihexyl-3,4-diphenyl-1-silole (**4b**) as previously reported using **2a** and **2b** as starting materials, respectively.[3,24] Briefly, intramolecular reductive cyclization, followed by *in situ* trimethylsilylation of **2a** and **2b** using lithium naphthalenide and trimethylchlorosilane afforded compounds **4a** and **4b,** respectively. The identity of **4a** and **4b** were confirmed using several spectroscopic methods. The ^{1}H NMR spectra of **4a** and **4b** exhibit multiplet peaks at 0.92–1.01 and 0.88–1.44 ppm, originated from the C$_2$H$_5$ and C$_6$H$_{13}$ groups, respectively.[35–37] The ^{13}C NMR spectra of **4a** and **4b** reveal two peaks at 5.21 and 7.29 ppm due to the C$_2$H$_5$ group directly bound to the silole Si atom, and six carbon peaks between 13.62 and 33.17 ppm due to the C$_6$H$_{13}$ group directly bound to the silole Si atom.[35–37] In the ^{29}Si NMR spectra of **4a** and **4b**, the silicon peak attached

Table 1. Some selected properties of silole derivatives **3a**, **3b**, **4a**, and **4b**.

Siloles	^{1}H NMR[a] δ (ppm)	^{13}C NMR[b] δ (ppm)	^{29}Si NMR[c] δ (ppm)	IR[d] $\nu_{(C=C)}$ (cm^{-1})	Absorption[e] $\lambda_{abs,\ max}$ (ε) (nm [cm^{-1} M^{-1}])	Excitation[f] $\lambda_{ex,\ max}$ (nm)	Fluorescence[g] $\lambda_{em,\ max}$ (nm)	Fluorescence FWHM[h] (nm)	CV[i]	TGA[j]
3a	1.04-1.09, 1.18–1.21, 7.00–7.02, 7.17–7.22	1.48, 6.54, 120.77, 127.36, 127.50, 128.95, 137.04, 157.22	8.521	1566	260 (1.19 × 10^4), 326 (3.50 × 10^3)	371	443	67	Epa +0.58 Epc −0.25	82.2
3b	0.91–1.01, 1.23–1.58, 6.95–6.97. 7.15–7.19	9.68, 14.15, 22.58, 22.85, 31.42, 32.68, 121.83, 127.35, 127.52, 128.95, 137.16, 156.78	6.176	1557	243 (1.28 × 10^4), 325 (2.63 × 10^3)	372	438	117	Epa +0.16 Epc −0.28	71.5
4a	−0.16, 0.92–0.96, 0.98–1.01, 6.82–6.84, 6.99–7.03	0.47, 5.21, 7.29, 125.93, 126.87, 128.83, 141.63, 143.09, 177.08	−10.04, 29.90	1543	303 (5.99 × 10^3)	356	424	93	Epa −0.45, −0.04 Epc −0.74, −1.12	96.1
4b	−0.15, 0.88–1.02, 1.27–1.44, 6.79–6.90, 6.96–7.11	0.64, 13.62, 14.20, 22.71, 23.89, 31.68, 33.17, 125.92, 126.85, 128.77, 142.73, 143.06, 170.52	−10.20, 26.56	1545	304 (5.50 × 10^2)	355	419	97	Epa −0.46, +0.14 Epc −0.69, −1.32	94.6

[a] In $CDCl_3$.

[b] In $CDCl_3$.

[c] In $CDCl_3$.

[d] Diene of silole ring in neat.

[e] In THF solution.

[f] Detection wavelengths 443, 438, 424, and 419 nm in THF solution for **3a, 3b, 4a**, and **4b**, respectively.

[g] Excitation wavelengths 371, 372, 356, and 355 nm in THF solution for **3a, 3b, 4a**, and **4b**, respectively.

[h] FWHM, full width at half maximum.

[i] Cyclic voltamogram. Epa, oxidation potential; Epc, reduction potential.

[j] Percentage weight remaining at 200 °C in nitrogen.

to the silole ring appeared at 29.90 and 26.56 ppm, respectively.[38]

The synthesized compounds were also characterized by FT-IR spectroscopy with the results summarized in Table 1. The FT-IR spectroscopic results of **3a**, **3b**, **4a**, and **4b** illustrated typical stretching frequencies of dienes within a silole ring between 1543 and 1566 cm^{-1}, illustrating that the conjugated dienes inside the silole ring remained intact throughout the trimethylsilylation reaction conditions.[39]

Photoelectronic Properties. We examined the photoelectronic properties of **3a**, **3b**, **4a**, and **4b** using absorption, excitation, and fluorescence measurements in tetrahydrofuran. Typical selected properties of siloles **3a**, **3b**, **4a**, and **4b** are listed in Table 1.

A representative absorption spectral trace of **3a** in tetrahydrofuran is shown in Figure 1 (—). The maximum absorption, $\lambda_{abs,max}$, of **3a** is found at 326 nm ($\varepsilon = 3.50 \times 10^3$/(cm.M)), with the trace reaching 396 nm. Similarly, the absorption spectra of materials **3b**, **4a**, and **4b** illustrate strong absorbance maxima ($\lambda_{abs,max}$) at 325, 303 and 304 nm, respectively, as shown in the Table 1. The strong absorption maxima in the UV–vis spectral traces of materials **3a**, **3b**, **4a**, and **4b** are due to the presence of chromophores, mainly the phenyl, as well as the diene functional groups within the 3,4-diphenyl-silole ring.[40]

The spectrophotometric excitation trace of **3a** showed a strong maximum, $\lambda_{ex,max}$, at 371 nm, using a 443 nm detection wavelength, λ_{det}, as depicted in Figure 1 (– –) and listed in Table 1. The excitation traces of **3b**, **4a**, and **4b** at the detection wavelengths 438, 424, and 419 nm, revealed strong excitation maxima at 372, 356, and 355 nm, respectively, as summarized in Table 1. The excitation bands in the spectral data of **3a**, **3b**, **4a**, and **4b** are ascribed to the chromophores of phenyl and diene groups in the 3,4-diphenyl-silole ring.[40]

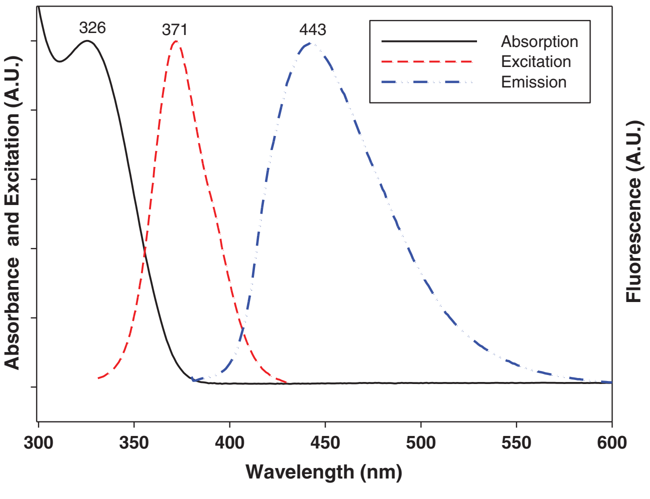

Figure 1. Absorbance, excitation, and fluorescence emission spectrophotometric traces of compound **3a** in THF.

The maximum fluorescence band, $\lambda_{em,max}$, observed at 443 nm in the fluorescence spectrum of **3a**, was obtained using an excitation wavelength, λ_{ex}, of 371 nm in THF, is depicted in Figure 1 (_.._) and listed in Table 1. The maximum fluorescence values, $\lambda_{em,max}$, for **3b**, **4a**, and **4b** measured using excitation wavelengths, λ_{ex}, of 372, 356, and 355 nm were 438, 424, and 419 nm, respectively, as summarized in Table 1. The strong emission peaks in the fluorescence emission spectra of the prepared siloles are attributed to the chromophores of phenyl and diene groups in the 3,4-diphenyl-silole ring.[40] Furthermore, the full widths at half maximum (FWHM) in the fluorescence spectra of **3a**, **3b**, **4a**, and **4b** were measured to be 67, 117, 93, and 97 nm, respectively, as listed in Table 1.

From the viewpoint of the excitation and fluorescence data we can speculate that the silole derivatives **3a**, **3b**, **4a**, and **4b** are comprised of chromophores contained within the silolene derivative, *i.e.*, 3,4-diphenyl-1-silacylopent-2,4-dienylene, phenyl and diene groups.[40] Furthermore, siloles with electron-releasing substituents, such as the Br atoms in **3a** and **3b**, show moderate bathochromic shifts (*i. e.*, 19–23 nm) of their absorption and fluorescence emission maxima in comparison to the trimethylsilyl substituted siloles, **4a** and **4b**.[41]

Cyclic Voltammetry Properties. We examined the cyclic voltammetric properties of compounds **3a**, **3b**, **4a**, and **4b** by coating the synthesized compounds onto copper electrodes. The working electrode copper film was fabricated by immersing a copper electrode into a hexane solution containing each of the synthesized compounds.

A representative CV of silole **3a** on a copper electrode immersed in an electrolyte bath of aqueous sulfuric acid solution (H_2SO_4, 1.0 M) is shown as trace (a) in Figure 2. The CV data for **3a** and **3b**, listed in Table 1, show an oxidation peak at 0.58 and 0.16 V vs. the Ag/Ag^+ reference electrode, respectively. Reduction peaks for **3a** and **3b** were observed at −0.25 and − 0.28 V vs. the Ag/Ag^+ reference electrode, respectively. On the basis of these results, the reduction may illustrate the transformation of **3a** and **3b** into their equivalent anions, for example [**3a**]$^-$ and [**3b**]$^-$, respectively. A similar phenomenon may occur for the reverse process of oxidation, involving the transformation of [**3a**]$^-$ and [**3b**]$^-$ anions back to **3a** and **3b**, respectively.[42,43]

The CV data for silole **4a** on a copper working electrode in an electrolyte bath of aqueous potassium hydroxide solution (KOH, 1.0 M) is illustrated as trace (b) in Figure 2. The CV data for **4a** and **4b**, listed in Table 1, reveals two oxidation peaks for each compound at −0.45, −0.04, and − 0.46, 0.14 V vs. the Ag/Ag^+ reference electrode, respectively. The two reduction peaks for each of **4a** and **4b** were observed at −0.74, −1.12, and − 0.69, −1.32 V, vs. the Ag/Ag^+ reference electrode, respectively. On the basis of these results, the reduction may illustrate the transformations of **4a** and **4b** into their equivalent anions, for example, [**4a**]$^-$, [**4a**]$^{-2}$, and [**4b**]$^-$, [**4b**]$^{-2}$, respectively.

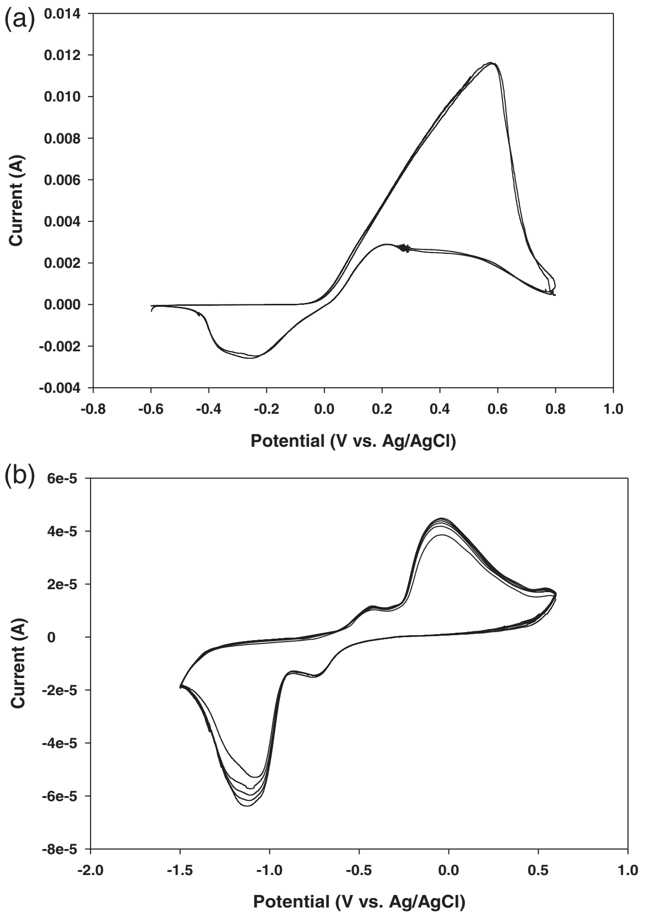

Figure 2. CV traces of (a) **3a** in an aqueous 1.0 M H_2SO_4 solution and (b) **4a** in an aqueous 1.0 M KOH solution.

Similarly, the reverse process of oxidation may involve the transformation of [**4a**]$^-$, [**4a**]$^{-2}$, and [**4b**]$^-$, [**4b**]$^{-2}$ anions back to **4a** and **4b**, respectively.[42,43] Furthermore, siloles with electron-releasing substituents, such as the Br atoms in **3a** and **3b**, show low-lying first oxidation potential levels, (*i.e.*, E_{pa}) in comparison with the trimethylsilyl substituted siloles **4a** and **4b**, respectively.[22]

The photoelectronic and cyclic voltammetric properties of **3a**, **3b**, **4a**, and **4b** illustrate the potential utility of the prepared silole derivative materials, specifically 1,1-diethyl or dihexyl-3,4-diphenyl-1-silacyclopenta-2,4-diene, in electrochemical device applications.

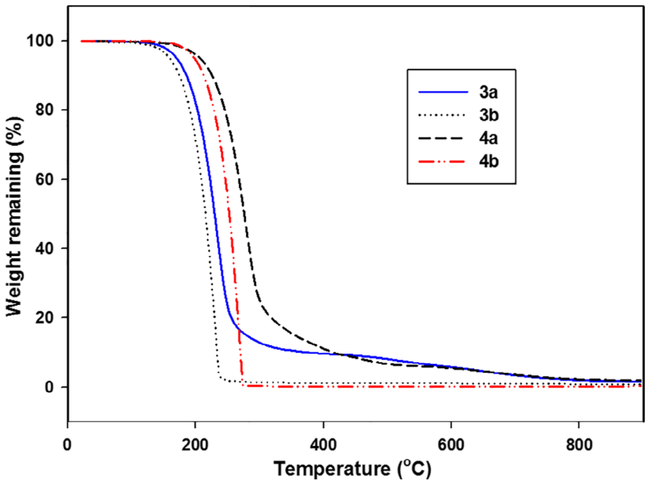

Figure 3. Thermogravimetric (TGA) traces of **3a**, **3b**, **4a**, and **4b** under nitrogen.

Thermal Properties. We examined the thermal stability of the siloles **3a**, **3b**, **4a**, and **4b** using a thermogravimetric analysis (TGA) system whereby the temperature was increased at a rate of 10 °C/min under a constant stream of nitrogen. The results are illustrated in Figure 3 and the data summarized in Table 1. The siloles **3a** and **3b** were found to be thermally stable up to 150 °C with less than a 2–3% decrease in their original masses under nitrogen. These siloles were found to suffer rapid losses in their mass when heated above 150 °C, with 85–95% of their initial mass lost between 150 and 300 °C. The loss of mass of the siloles is attributed to the thermal decomposition of functional groups on the silole ring, for example, the phenyl, bromine, ethyl, and hexyl functionalities.[37] Between temperatures of 600 and 900 °C an additional 0.3–4% of their initial masses were lost.

The siloles **4a** and **4b** were very thermally stable up to 150 °C with only a 0.3–0.7% decrease in their original masses under nitrogen being observed. These siloles were found to suffer rapid losses in their mass when heated above 150 °C, with 88 to 99% of their initial mass lost between 150 and 400 °C. The loss of mass of the siloles is attributed to thermal decomposition of functional groups on the silole ring, *e.g.*, the phenyl, trimethylsilyl, ethyl, and hexyl functionalities.[37] Between temperatures of 600 and 900 °C an additional 0.1–9% of their initial masses were lost.

In summary, each of the siloles **3a**, **3b**, **4a**, and **4b** were thermally stable under nitrogen up to 150 °C with less than 0.3–3% losses of the initial mass observed, and 72–96% of their initial mass remaining at 200 °C under N_2 atmosphere. These results are illustrated in Figure 3 and summarized in Table 1.

Long Cycling Performance Property. We examined the long cycling performance properties of the anode silole materials **4a** and **4b** at 1 A/g current density, as guided by their CV data in Figure 4.

For the anode silole material **4a**, the first discharge/charge capacity was found to be 1967/754 mAh/g with 38.2% Coulomb efficiency at 20 cycles followed by a 908 mAh/g charge capacity with 46.1% Coulomb efficiency achieved after 105 cycles. Subsequently, the charge capacity of the anode material **4a** slowly decreased to 517 mAh/g with 26.2% Coulomb efficiency after 1000 cycles.

For the anode material **4b**, the initial discharge/charge capacity was found to be 5559/1174 mAh/g with a lower Coulomb efficiency of 21.1% at 15 cycles followed by a

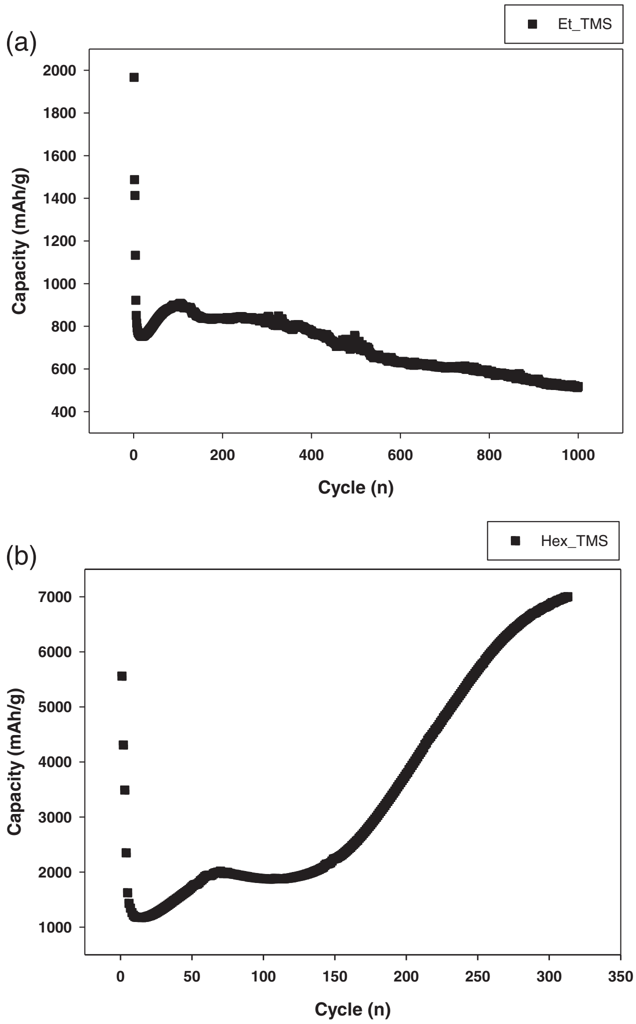

Figure 4. Long cycling performances of the anodes **4a** and **4b**.

2019 mAh/g charge capacity with 36.3% Coulomb efficiency achieved after 70 cycles. Subsequently, the charge capacity of anode **4b** slowly increased to 5674 mAh/g with 102% Coulomb efficiency at 250 cycles and was observed to continuously increase to 7002 mAh/g with 126% Coulomb efficiency at 313 cycles.

Conclusion

Here we report the synthesis of 2,5-dibromo-siloles **3a**, **3b**, and 2,5-bis(trimethylsilyl)-siloles **4a**, **4b**. All four of the silole derivatives prepared dissolved very well in common solvents such as tetrahydrofuran and chloroform. We studied the spectrophotometric properties of the siloles using a variety of techniques. FT-IR traces of all the silole derivatives illustrated the expected stretching bands of diene functional groups at 1543–1566 cm^{-1}. Silole derivatives in tetrahydrofuran solutions showed absorption maxima at 303–326 nm, excitation bands at 355–372 nm, and fluorescence emission peaks at 419–443 nm. The experimental absorption, excitation, and emission data illustrated that all the silole derivatives are composed of the expected chromophores, for example, phenyl and 1,4-diene of 3,4-diphenyl-1-silacyclopenta-2,4-dienylene, within the silole skeleton. CVs of **3a** and **3b** revealed oxidation peaks at 0.58 and 0.16 V, and reduction peaks at −0.25 and −0.28 V, respectively. CVs of **4a** and **4b** revealed two oxidation peaks ranging from −0.46 to 0.14 V, as well as two reduction peaks ranging from −1.32 to −0.69 V. TGA revealed that all siloles were thermally stable up to 150 °C suffering only a 0.3 to 3% loss of their original masses under nitrogen. Finally, the long cycling performance of anodes **4a** and **4b** exhibited initial discharge/charge capacities, at a 1 A/g current density, of 1967/754 with 38.2% Coulomb efficiency at 20 cycles, and 5559/1174 mAh/g Coulomb efficiency of 21.1% at 15 cycles, respectively. The photoelectronic and electrochemical characteristics of **4a** and **4b** confirms their utility for applications in novel electronic materials.

Acknowledgment. This research was supported by the National Research Foundation of Korea (NRF) funded by the Ministry of Education of the Republic of Korea (NRF-2017R1D1A3B03028014).

Supporting Information. All spectroscopic data including NMR, IR, and UV–vis, along with TGA traces for the compounds **2a**, **2b**, **3a**, **3b**, **4a**, and **4b** are available in the online version of this article.

References

1. (a) E. H. Braye, W. Hübel, *Chem. & Ind. (London, U. K.)* **1959**, 1250. (b) E. H. Braye, W. Hübel, I. Caplier, *J. Am. Chem. Soc.* **1961**, *83*, 4406.
2. J. Dubac, A. Laporterie, G. Manuel, *Chem. Rev.* **1990**, *90*, 215.
3. S. Yamaguchi, K. Tamao, *J. Chem. Soc. Dalton Trans.* **1998**, *22*, 3693.
4. W. Chen, S. Ijadi-Maghsoodi, T. Barton, *Polym. Prepr. (Am. Chem. Soc., Div. Polym. Chem.)* **1997**, *38*, 189.
5. S. Yamaguchi, K. Limura, K. Tamao, *Chem. Lett.* **1998**, *27*, 89.
6. A. J. Boydston, Y. Yin, B. L. Pagenkopf, *J. Am. Chem. Soc.* **2004**, *126*, 10350.
7. S. Yamaguchi, K. Tamao, *Chem. Lett.* **2005**, *34*, 2.
8. K. Tamao, S. Yamaguchi, M. Shiro, *J. Am. Chem. Soc.* **1994**, *116*, 11715.
9. J. Oshita, N. Mimura, H. Arase, M. Nodono, A. Kunai, K. Komaguchi, M. Shiotani, *Macromolecules* **1998**, *31*, 7985.
10. M. S. Liu, J. Luo, A. K.-Y. Jen, *Chem. Mater.* **2003**, *15*, 3496.
11. Z. Liu, J. Zou, J. Chen, Y. Cao, *Polym. Prepr. (Am. Chem. Soc., Div. Polym. Chem.)* **2009**, *50*, 485.
12. Z. Zhao, D. Liu, F. Mahtab, L. Xin, Z. Shen, Y. Yu, C. Y. K. Chan, P. Lu, J. W. Y. Lam, H. H. Y. Sung, I. D. Williams, B. Yang, Y. Ma, B. Z. Tang, *Chem. Eur. J.* **2011**, *17*, 5998.
13. T. Sanji, T. Sakai, C. Kabuto, H. Sakurai, *J. Am. Chem. Soc.* **1998**, *120*, 4552.

14. J. Chen, B. Xu, K. Yang, Y. Cao, H. Sung, I. Williams, B. Tang, *J. Phys. Chem.* **2005**, *109*, 17086.
15. K. Geramita, J. McBee, Y. Shen, N. Radu, T. Tilley, *Chem. Mater.* **2006**, *18*, 3216.
16. C. Ding, G. Babu, A. Orita, T. Hirate, J. Otera, *Synlett* **2007**, *16*, 2559.
17. C. K. W. Jim, R. Hu, M. Faisal, J. W. Y. Lam, B. Z. Tang, *Polym. Prepr. (Am. Chem. Soc., Div. Polym. Chem.)* **2011**, *52*, 842.
18. Y. T. Park, *Bull. Kor. Chem. Soc.* **2016**, *37*, 56.
19. H. Usta, G. Lu, A. Facchetti, T. J. Marks, *J. Am. Chem. Soc.* **2006**, *128*, 9034.
20. H.-J. Son, W.-S. Han, H. Kim, C. Kim, J. Ko, C. Lee, S. O. Kang, *Organometallics* **2006**, *25*, 766.
21. S. Yamaguchi, R.-Z. Jin, Y. Itami, T. Goto, K. Tamao, *J. Am. Chem. Soc.* **1999**, *121*, 10420.
22. S. Yamaguchi, K. Tamao, In *The Chemistry of Organic Silicon Compounds*, Vol. *3*, Z. Rappoport, Y. Apeloig Eds., John Wiley & Sons, Chichester, **2001**, Chapter 11.
23. J. Chen, Y. Cao, *Macromol. Rapid Commun.* **2007**, *28*, 1714.
24. Y. T. Park, *Bull. Kor. Chem. Soc.* **2014**, *35*, 1825.
25. a Y. M. Jung, S.-H. Baek, Y. T. Park, *Bull. Kor. Chem. Soc.* **2017**, *38*, 91. b J. H. Jang, Y. T. Park, *Bull. Kor. Chem. Soc.* **2018**, *39*, 313.
26. Y. M. Jung, J. H. Jang, Y. T. Park, *Bull. Kor. Chem. Soc.* **2019**, *40*, 192.
27. M. Armand, J.-M. Tarascon, *Nature* **2008**, *451*, 652.
28. X. Wang, X. Lu, B. Liu, Y. Tong, G. Shen, *Adv. Mater.* **2014**, *26*, 4763.
29. H. H. Lee, Y. Park, K.-H. Shin, K. T. Lee, S. Y. Hong, *ACS Appl. Mater. Interfaces* **2014**, *6*, 19118.
30. Z. Lei, Q. Yang, Y. Xu, S. Guo, W. Sun, H. Liu, L.-P. Lv, Y. Zhang, *Nat. Commun.* **2018**, *9*, 576.
31. H. Kinoshita, H. Fukumoto, A. Ueda, K. Miura, *Tetrahedron* **2018**, *74*, 1632.
32. Y. J. Cho, S. Y. Kim, J. W. Lee, W. S. Han, C. H. Kim, H. J. Son, S. O. Kang, *Chem. Eur. J.* **2019**, *25*, 1.
33. C. N. Scott, M. D. Bisen, *Polymer* **2019**, *170*, 204.
34. W. L. F. Armarego, D. D. Perrin, *Purification of Laboratory Chemicals*, 4th ed., Butterworth-Heinemann, Oxford, **1996**.
35. N. A. Morra, B. L. Pagenkopf, *Org. Synth.* **2008**, *85*, 53.
36. E. Pretsch, P. Bühlmann, C. Affolter, *Structure Determination of Organic Compounds, Tables of Spectral Data*, 3rd ed., Springer-Verlag, Berlin, **2000**.
37. R. M. Silverstein, F. X. Webster, D. J. Kiemle, *Spectrometric Identification of Organic Compounds*, 7th ed., John Wiley & Sons, Hoboken, NJ, **2005**.
38. E. A. Williams, In *The Chemistry of Organic Silicon Compounds*, S. Patai, Z. Rappoport Eds., Wiley, Chichester, **1989**, p. 1, Chapter 8.
39. L. J. Bellamy, *The Infra-Red of Complex Molecules*, 3rd ed., John Wiley and Sons, New York, **1975**.
40. N. N. Barashkov, O. A. Gunder, *Fluorescent Polymers*, Ellis Horwood, London, **1994**.
41. D. L. Pavia, G. M. Lampman, G. S. Kriz, *Introduction to Spectroscopy, A Guide for Students of Organic Chemistry*, 3rd ed., Brooks/Cole Thomson Learning, Inc., Washington, DC, **2001**.
42. H. Maruyama, H. Nakano, M. Nakamoto, A. Sekiguchi, *Angew. Chem.* **2014**, *126*, 1348.
43. Y. Chen, S. Zeng, J. Qian, Y. Wang, Y. Cao, H. Yang, X. Ai, *Appl. Mater. Interfaces* **2014**, *6*, 3508.